JAEHR
Journal of Advances in Environmental Health Research
J Adv Environ Health Res. 2025;13(3):183-190. doi: 10.34172/jaehr.1392
http://jaehr.muk.ac.ir

Original Article

Cadmium Sulfide-Modified Carbon Nitride/Graphite for Photocatalytic Removal of Sulfamethoxazole From Aqueous Solutions

Ali Esrafily[1,2], Hossein Pasavand[3*], Mehdi Safari[4], Majid Kermani[1,2]

[1]Department of Environmental Health Engineering, School of Public Health, Iran University of Medical Sciences, Tehran, Iran
[2]Research Center for Environmental Health Technology, Iran University of Medical Sciences, Tehran, Iran
[3]Department of Environmental Health Engineering, School of Health, Iran University of Medical Sciences, Tehran, Iran
[4]Department of Environmental Health Engineering, School of Health, Kurdistan University of Medical Sciences, Kurdistan, Iran

Article history:
Received: August 6, 2024
Revised: November 19, 2024
Accepted: December 31, 2024
ePublished: September 27, 2025

***Corresponding author:**
Hossein Pasavand,
Email: hosseinpasavand@gmail.com

Abstract

Background: Sulfamethoxazole (SMX), a sulfonamide antibiotic, is frequently detected at high concentrations in surface and drinking water, indicating widespread contamination.

Methods: In this experimental study, a graphitic carbon nitride (g-C_3N_4)/cadmium sulfide (CdS) nano-composite was synthesized using a co-precipitation method. The crystal structure, morphology, and surface chemistry of the synthesized nanocomposite were characterized using X-ray powder diffraction (XRD), field emission scanning electron microscopy (FE-SEM), and energy-dispersive X-ray spectroscopy (EDX), respectively. The Experiments were conducted under varying conditions, including pH (3–11), nanocatalyst dosage (0.2–1 g/L), contact time (0–120 minutes), and initial SMX concentration (5–20 mg/L).

Results: XRD and SEM analyses confirmed the hexagonal structure of CdS, with SEM images showing well-dispersed nanoparticles and no agglomeration. The distinct peaks in the XRD pattern indicated well-crystallized CdS nanoparticles. Optimal removal efficiency was achieved at pH 5, with a nanocatalyst dosage of 0.7 g/L, a contact time of 60 minutes, and an SMX concentration of 5 mg/L. Kinetic studies revealed that the photocatalytic degradation followed first-order kinetics ($R^2 = 0.9955$).

Conclusion: Based on the results and the physical and chemical properties of the synthesized CdS-modified carbon nitride nanocomposite, this photocatalytic process offers a promising, effective, and efficient method for the treatment of antibiotic-contaminated wastewater, particularly for removing SMX.

Keywords: Sulfamethoxazole, Photocatalyst, Cadmium sulfide, Carbon nitrite graphite, Purification

Please cite this article as follows: Esrafily A, Pasavand H, Safari M, Kermani M. Cadmium sulfide-modified carbon nitride/graphite for photocatalytic removal of sulfamethoxazole from aqueous solutions. J Adv Environ Health Res. 2025; 13(3):183-190. doi: 10.34172/jaehr.1392

Introduction

Among various classes of pharmaceuticals, antibiotics are the most widely consumed worldwide.[1] However, their overuse and increasing rates of consumption have reduced their effectiveness against bacteria.[2] This growing inefficacy is further complicated by the rising costs of medical and veterinary care, the development of antibiotic resistance in humans,[3,4] and the high potential for mutations in microorganisms, which can lead to even greater resistance.[1] Moreover, antibiotics are also toxic and non-biodegradable in the environment.[5] Their presence can negatively impact biological wastewater treatment processes and may interfere with chemical treatment methods such as chlorination and ozonation, potentially leading to the formation of even more toxic byproducts.[6] These byproducts can subsequently affect living organisms—humans, animals, and plants—by adsorbing onto target cells[6]. The high solubility of antibiotics in water facilitates the rapid contamination of water resources, including drinking water, surface water, and groundwater.[6-8] This contamination can ultimately harm the environment and contribute to the emergence of antibiotic-resistant bacteria. Among antibiotics, sulfamethoxazole (SMX)—a sulfonamide compound—is widely used to treat urinary tract infections and respiratory illnesses such as bronchitis, and is also extensively used in veterinary medicine.[9] This widespread application is a likely cause of high SMX concentrations detected

in surface and drinking water.[10] Due to its frequent detection, SMX is often considered a key indicator of antibiotic pollution in aquatic environments.[11] It enters water bodies through multiple pathways, including medical waste discharge, toilet flushing, and improper disposal from both industrial and domestic sources.[11] Notably, SMX has low biodegradability, allowing it to persist in the environment, thus classifying it as a stable contaminant.[12] Given its toxicological effects on aquatic ecosystems and potential human health risks, even low levels of SMX in wastewater must be effectively removed.[13] However, conventional wastewater treatment processes are not effective in removing antibiotics from wastewater,[14] necessitating the development of novel and effective removal methods. Various techniques have been applied to eliminate SMX from aqueous environments, including adsorption, anaerobic digestion, cavitation, ion exchange, photo-Fenton oxidation, catalytic oxidation under radiation, and photocatalysis.[14-16] While Fenton oxidation and photocatalytic degradation are among the most commonly employed, the generation of large amounts of iron sludge remains a significant limitation of the Fenton process. As a result, photocatalytic degradation is increasingly favored for the effective removal of antibiotics like SMX.[17]

Cadmium sulfide (CdS) is a semiconductor of considerable interest owing to its bandgap of approximately 2.4 eV, which enables it to effectively absorb sunlight up to around 520 nm.[18] It exhibits strong visible light absorption, favorable energy band positions, and excellent electron transport properties, making it well-suited for the removal of hazardous contaminants.[19] However, CdS in its untreated form suffers from considerable electron-hole recombination and photocorrosion during photocatalytic processes, which limits its effectiveness in detoxifying pollutants.[20]. Graphene, known for its outstanding physicochemical properties—such as high electrical conductivity, chemical stability, and strong light absorption—serves as an effective cocatalyst for rapid reactions.[21] Its characteristics facilitate the efficient collection and transport of charge carriers, enhancing overall reaction efficiency and longevity.[21] Graphitic carbon nitride (g-C_3N_4) is another promising organic, metal-free semiconductor known for its strong thermal and structural stability, scalability, low toxicity, appropriate band structure, and cost-effectiveness.[22, 23] Nevertheless, g-C_3N_4 alone is limited by its poor ability to separate photo-induced electron-hole pairs at the interface, which restricts its photocatalytic efficiency.[23]. The integration of CdS nanomaterials with graphene—particularly at key interfaces—can significantly improve charge separation and transfer efficiency.[24] Furthermore, g-C_3N_4's large surface area and suitable band structure, which is lower than many conventional semiconductors, underscore its potential when used in heterojunction photocatalysts in combination with other materials.[25] The resulting CdS/graphene/g-C_3N_4 photocatalysts are particularly promising for the efficient degradation of organic pollutants. In addition to their enhanced photocatalytic performance, these composites can be easily recovered from aquatic environments via simple sedimentation, making them highly practical for real-world applications.

In this study, a novel g-C_3N_4/CdS nanocomposite photocatalyst was synthesized using the co-precipitation method. The CdS nanoparticles were prepared following established procedures reported in previous studies. The synthesized materials were characterized using energy-dispersive X-ray (EDX) analysis, scanning electron microscopy (SEM), and X-ray Diffraction (XRD) to determine their elemental composition, surface morphology, and crystal structure, respectively. The photocatalytic performance of the nanocomposite was evaluated by investigating key operational parameters, including pH, irradiation time, and initial SMX concentration. Additionally, the reaction kinetics of SMX degradation were analyzed to better understand the efficiency and mechanism of the photocatalytic process.

Methods and Materials

This research involved practical experiments conducted on a bench scale using a batch reactor.

Instruments and Materials

All chemicals used in this study—including hydrochloric acid, sulfuric acid, sodium hydroxide, cadmium nitrate tetrahydrate ($Cd(NO_3)_2{\cdot}4H_2O$), thiourea ($CS(NH_2)_2$), and silver nitrate ($AgNO_3$)—were of analytical grade and obtained from Merck. These chemicals were used as received, without any further purification. The physical and chemical properties of SMX, the target antibiotic (purchased from Sigma-Aldrich), are summarized in Table S1.

Synthesis of G-C_3N_4/CdS

All materials used for the synthesis of the nano-composite were commercially available and did not require further refinement. The G-C_3N_4/CdS nanocomposite was synthesized using a co-precipitation method.[27,28] The G-C_3N_4 sample was prepared by heating melamine directly at 520 °C for 4 hours in a semi-closed system. To synthesize the G-C_3N_4-CdS composites, a mixture of $Cd(NO_3)_2{\cdot}4H_2O$ and thiourea in a 2:1 molar ratio was dissolved in 50 mL of distilled water after stirring for 30 minutes. A specific amount of G-C_3N_4 powder was then added to this solution, which was shaken for 3 hours. The pH of the resulting suspension was subsequently adjusted to 10 by adding 0.5 M NaOH, and the reaction was maintained for 12 hours under constant stirring. After the reaction, the deposited material was collected by filtration, washed thoroughly with distilled water, and dried overnight at 60 °C. Finally, the sample was heated at 250 °C for 1 hour.

Structure and Morphology of G-C_3N_4/CdS

The crystallization and particle size of G-C_3N_4-CdS were analyzed using XRD patterns over the range of 5 to 80 degrees with a Phillips X-ray machine (X-ray tube anode: copper, wavelength: 1.540598 Å [Cu-Kα], filter: Ni). The photocatalytic surface morphology of g-C_3N_4-CdS was characterized using a FE-SEM TESCAN MIRA3. Also, EDX analysis was employed to examine the elemental composition of the photocatalyst. The point of zero charge (pzc) of the catalyst was evaluated based on its properties, particularly the surface charge determined by the ions present on the catalyst's particle structure.[29] To investigate the impact of pH on the photocatalytic degradation of pollutants and the dependence of pzc on the solution's pH, the pHpzc of the synthesized G-C_3N_4/CdS was determined. To estimate pHpzc, 30 mL of a 0.01 M sodium chloride suspension was placed into five 100 mL Erlenmeyer flasks, and the solutions were adjusted to pH levels ranging from 2 to 11 using 0.1 M HCl and NaOH. Subsequently, 0.2 g of the nanocatalyst was added to each flask, which were then shaken at 200 rpm for 48 hours. The final pH of each sample was measured, and pHpzc was deduced from the intersection point of the initial pH graph versus the final Ph.[29,30] The pHpzc was determined to be 5.4. For pH levels below the pHpzc, the surface of the nanoparticles exhibits a positive electrical charge due to the presence of H^+ ions. Conversely, at pH levels above the pHpzc, the surface charge becomes negative owing to the presence of OH^- ions.[30] (Figure 1)

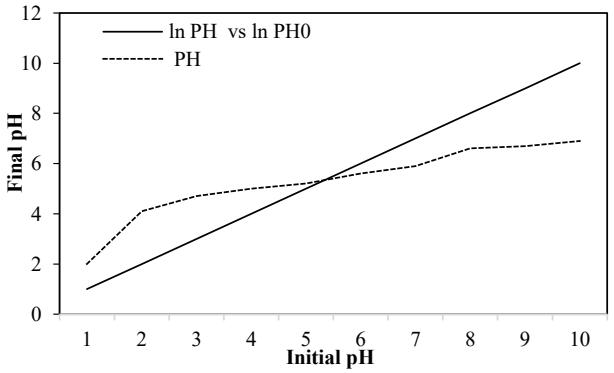

Figure 1. Zero-Point Charge of the Prepared G-C_3N_4/CdS Nanocatalyst in This Study

Study of the Photocatalytic Process in SMX Removal

The experimental studies were carried out in a cylindrical batch reactor with a height of 127 mm, a diameter of 85 mm, and a total volume of 720 cm^3. For each experiment, the reactor was filled with 500 mL of distilled water. The schematic of the experimental setup is shown in Figure S1.

Different experimental samples were prepared by adding the appropriate amounts of sulfamethoxazole and the nanocatalyst. The suspension was allowed to sit in the dark for 30 minutes to reach adsorption/desorption equilibrium. The reactor was then exposed to a UV light source, a 15 W low-pressure UV lamp with specified irradiation intensity, positioned in the center of the reactor and covered with quartz to prevent direct contact between the lamp and the solution. Throughout the reaction, the magnetic stirrer was kept constant, and the temperature of the solution was maintained. The entire reactor was wrapped in aluminum foil to prevent light reflection. Samples of 5 mL were continuously withdrawn from the reactor, and the solution containing the photocatalyst was centrifuged at 6000 rpm for 30 minutes to separate the particles. The supernatant was then passed through a 0.5 µm filter to remove any remaining photocatalyst. The residual concentration of SMX was measured using a spectrophotometer at a wavelength of 270 nm.[31] The highest efficiency was used to determine the optimal conditions for various operational parameters.

Impact of pH

The effect of initial pH on the photocatalytic removal of SMX was investigated over a pH range of 3 to 11 at specified time intervals. The experiments were carried out using an initial SMX concentration of 5 mg/L and a nanocatalyst dosage of 0.5 g/L under UV light irradiation.

Impact of Nanocatalyst Dosage

The effect of varying nano-catalyst dosages (0.2–1 g/L) on the degradation of SMX was investigated at specified time intervals, while maintaining optimal pH conditions and a constant SMX concentration of 5 mg/L under UV light irradiation.

Impact of Initial SMX Concentration

The effect of the initial concentration of SMX (ranging from 5 to 20 mg/L) on its photocatalytic degradation was examined at specific time intervals, using optimal pH and the optimal nanocatalyst dosage under UV light irradiation.

Impact of Reaction Time

The effect of reaction time (0–120 minutes) on the photocatalytic degradation of SMX was investigated under UV light irradiation, using the optimal SMX concentration, pH, and nanocatalyst dosage.

Photocatalytic Removal Kinetics

The kinetics of photocatalytic degradation of SMX were studied at the optimal SMX concentration, optimal reaction time, optimal pH, and optimal dosage of nanocatalyst under a UV light source.

Removal Efficiency Calculation

The removal efficiency of SMX was calculated by equation 1:

$$\%\mu = \frac{Ci - Cf}{Ci} \times 100 \quad (1)$$

Where, Ci is the initial concentration of SMX and C_f is the final concentration of SMX (mg/L).

Results and Discussion

Characterization of G-C_3N_4-CdS Heterojunctions

As shown in the XRD diagram (Figure 2), the main peaks of CdS were observed at 26.7°, 44.1°, and 52.2°, with a smaller peak at 70.8° corresponding to the planes (002, 111) and (220, 311, 331). Moreover, a minor peak at 24.9° was associated with the crystal plane (100), confirming the hexagonal crystal structure of CdS.[32,33] The peaks corresponding to G-C_3N_4 included the integrated peaks of CdS and G-C_3N_4 together, with a broad and sharp peak at 27.47°, indicative of the layered arrangement within the graphite-like carbon nitride. Another peak was observed at 13.04°, confirming the arrangement of the triazine structures on the surface of the conjugated aromatic systems, which is responsible for the formation of G-C_3N_4.[33]

The FE-SEM results show that CdS nanoparticles are dispersed on the G-C_3N_4 plates (Figure S2). The hexagonal CdS particles were well deposited on both the inner and outer surfaces of the G-C_3N_4 plates, which is consistent with findings from other studies.[32,33] According to Chen et al, g-C_3N_4 exhibits two characteristic diffraction patterns, attributed to the in-plane structural arrangement and the interlayer stacking of aromatic layers in graphitic materials.[33] In this study, these diffraction features were also utilized. Elemental analysis revealed the presence of the constituent elements in the nanocomposite, including carbon (C), nitrogen (N), sulfur (S), and cadmium (Cd). The weight ratios of these elements were 30.4% for C, 40.2% for N, 14.1% for S, and 15.3% for Cd. The weight ratio of Cd to S was approximately 1.08, indicating the formation of CdS. Furthermore, the analysis showed that the nanocomposite contained 30% of the total nanoparticles, with only the peaks for these constituent elements appearing in the graph, indicating the absence of impurities from other elements in the desired photocatalyst.

Photocatalytic study of G-C^3N^4/CdS heterojunctions

To achieve the highest removal efficiency of SMX from the aqueous solution, the roles of various influencing parameters were investigated, including nanocatalyst dosage, initial SMX concentration, initial pH, and reaction time. The kinetics of SMX removal through photocatalysis were also studied.

Impact of initial pH

pH is one of the most influential parameters for the removal of antibiotics in photocatalytic processes.[34] It plays a crucial role in the photocatalytic decomposition of pollutants by affecting the concentration of H^+ and OH^- ions in solution.[34] pH directly impacts the production of reactive species, such as photogenerated holes and the formation of superoxide and hydroxyl radicals, as well as surface chemistry, including photocatalytic surface charge, pollutant reactivity, and electrostatic interactions between the pollutant and photocatalyst.[3,4,30,34]

In this study, the degradation rate of the antibiotic SMX was investigated under acidic, neutral, and basic conditions. The results showed that the removal efficiency of SMX increased with pH, reaching its highest value at pH 5 (Figure 3). Beyond this point, further increases in pH led to a decrease in efficiency. Song et al reported that as pH increases, the oxidizing potential of photo-generated holes tends to decrease, likely due to a reduction in electropositivity.[35] This reduction in oxidizing potential could lead to lower photodegradation efficiency, a trend that appears relevant to the present study. As the pH increased beyond 5, the SMX removal efficiency declined, with the lowest efficiency observed at pH 11. This trend can be explained by the point of zero charge (pHzpc = 5.4) of the photocatalyst, indicating that the catalyst surface is positively charged under acidic conditions and negatively charged under alkaline conditions.[34] Besides, since SMX contains a negatively charged sulfonamide group, it is attracted to the positively charged photocatalyst in acidic solutions, enhancing the efficiency of optical degradation.[36] Furthermore, the acidic dissociation constants of sulfamethoxazole are $pKa_1 = 1.6$ and $pKa_2 = 5.7$. This means that at pH < 1.7, SMX exists predominantly as a cation; between pH 1.7 and 5.6, it remains mostly in a neutral form; and at pH > 5.6, it is primarily anionic. These findings indicate that SMX can be effectively removed under near-neutral conditions, where electrostatic interactions between SMX and the G-C_3N_4/CdS photocatalyst are minimized. According to Boreen et al, neutral SMX exhibits stronger light absorption and a higher photochemical reaction rate, leading to a shorter

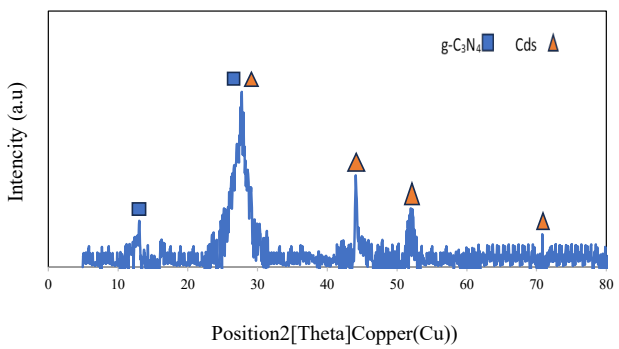

Figure 2. XRD Pattern of the G-C_3N_4-CdS Synthesized in This Study

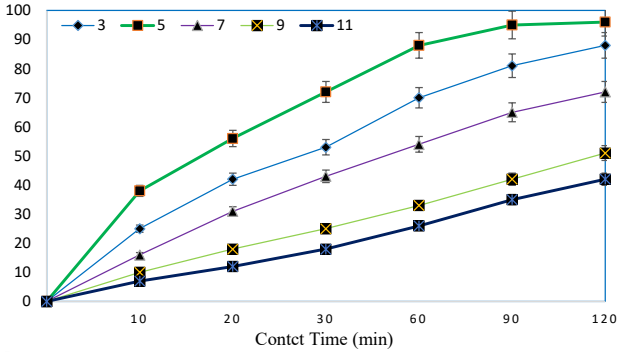

Figure 3. Effect of initial pH on the removal efficiency of SMX

half-life and enhanced degradation efficiency.[37]

Impact of Photocatalyst Dosage

Catalyst dosage is a critical parameter that must be carefully optimized for each treatment method, as the optimal dosage ensures high efficiency while keeping operational costs low. The required amount of photocatalyst depends on several factors, including the type of catalyst, reactor dimensions, and the nature of the pollutant present in the aquatic environment.[4] Generally, higher concentrations of catalysts create more active sites, leading to an increased rate of reactive radical production.[35] In this study, the efficiency of various dosages of the G-C_3N_4/CdS photocatalyst (0.2, 0.5, 0.7, and 1 g/L) for the removal of SMX was investigated. As shown in Figure 4, SMX removal efficiency increased from 43% to 87% as the dosage of G-C_3N_4/CdS increased from 0.2 g/L to 0.7 g/L over 60 min. This indicates that a higher photocatalyst dosage enhances the reaction rate and, consequently, the removal efficiency. However, while increasing the dosage to 0.7 g/L improved efficiency, further increases in dosage led to a decline in performance. This reduction can be attributed to the increased suspended matter in the solution, which raises turbidity and leads to agglomeration of the photocatalyst particles.[35] As turbidity increases, the absorption of light by the particles diminishes, reducing the penetration of light and subsequently decreasing the production of free radicals and overall efficiency.[38] A similar trend was reported by Khataee et al, where the degradation efficiency increased from 14 to 57% as the catalyst dosage rose from 0.25 to 1 g/L but decreased to 50% when the dosage was raised to2 L.[39] These observations are consistent with the results of the present study.

Impact of Initial SMX Concentration

The initial concentration of the pollutant is an important parameter due to its impact on the optimal dosage of catalyst required for photocatalytic degradation.[39] In this study, we investigated the effect of initial SMX antibiotic concentrations (5, 10, and 20 mg/L) on removal efficiency using the G-C_3N_4/CdS photocatalyst. As shown in Figure 5, the removal efficiency of SMX varied with different initial concentrations. The lowest removal efficiency (44%) was observed at a concentration of 20 mg/L after 60 minutes. In contrast, the removal efficiency increased as the initial concentration decreased, with the highest efficiency (92%) noted at a concentration of 5 mg/L. This indicates that SMX degradation decreased with increasing initial concentration. Moreover, while the concentration of the nanocatalyst—and therefore the number of active sites for the production of reactive radicals—remained constant, a higher number of contaminants absorbed by the nanocatalyst can reduce the availability of reactive sites, subsequently lowering removal efficiency.[6,35,39] At higher initial concentrations, the absorption of SMX onto the photocatalyst has an inhibitory effect on the reaction of SMX molecules with the photogenerated holes and hydroxyl radicals.[40] Also, increasing the concentration of SMX can scatter and absorb optical photons, preventing them from reaching the photocatalyst surface, which reduces the production of reactive radicals and diminishes degradation efficiency.[40] Another possible reason for the reduced efficiency at higher antibiotic concentrations is the increased presence of by-products and intermediates, which compete with antibiotic molecules for the limited active sites on the photocatalytic surface, further decreasing SMX removal efficiency.[41,42]

Impact of Reaction Time

Reaction time is one of the most important parameters affecting pollutant removal; as time increases, the photocatalyst has more opportunities to eliminate pollutants, resulting in a direct relationship between time and removal efficiency. As illustrated in Figure 6, the SMX removal efficiency increased from 46% to 92% when the reaction time was extended from 10 to 60 min, with 60 min identified as the optimal reaction time. In addition, as the reaction time increased, the rate of improvement in removal efficiency began to level off, indicating a lower slope in the efficiency increase.[43] The initial rise in removal efficiency can be attributed to the formation of more active sites and reactive radicals, which enhances the overall removal efficiency.[17,35,43] Longer reaction times allow for greater exposure of the photocatalyst to light, leading to increased catalyst activation and, consequently,

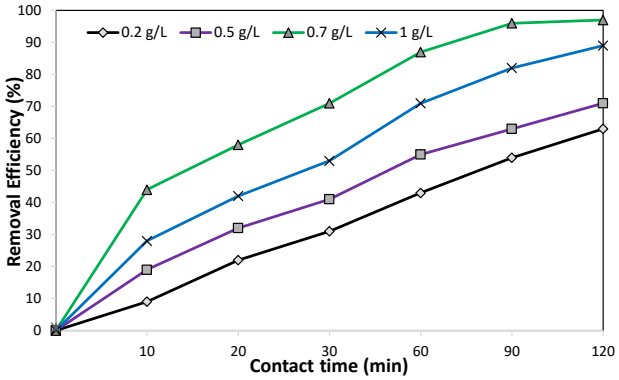

Figure 4. Effect of G-C_3N_4-CdS Dosage on SMX Removal Efficiency

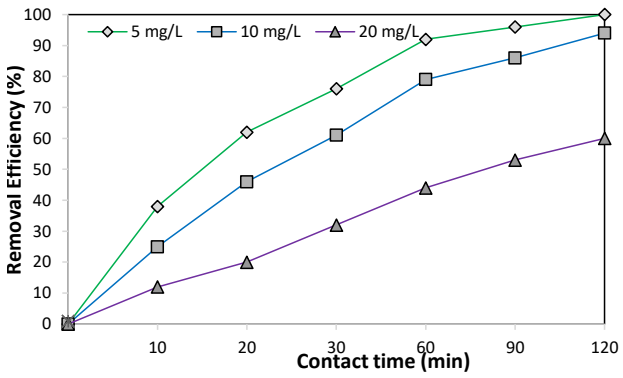

Figure 5. Effect of Initial SMX Concentration on Removal Efficiency

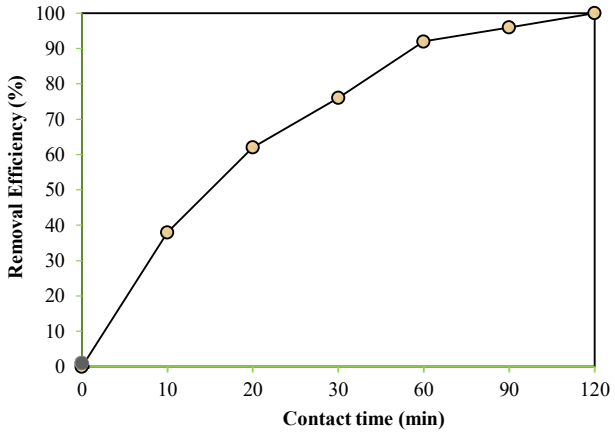

Figure 6. Effect of Contact Time on Photocatalytic Removal of SMX

improved removal efficiency. It is important to note that SMX is known to be a recalcitrant compound, meaning that efficient removal requires more time. Extended reaction times enhance oxidation-reduction potentials, producing more active hydroxyl radicals and providing sufficient opportunities for these radicals to react with the antibiotic.[35]

SMX photocatalytic Removal Kinetic

Kinetics play a crucial role in selecting and designing processes, as they influence reaction speed and the control of stoichiometric conditions.[3,17] The correct application of kinetic models to interpret experimental data is essential for designing and optimizing a system with adequate capacity and minimal non-radiant volume in the reactor. The rate of a reaction is generally affected by the initial concentration of the pollutant or product over time.[39] In this study, we first determined the degree of SMX removal efficiency (Figure S3). The results indicated that the SMX removal efficiency followed first-order kinetics ($R^2 = 0.99$), suggesting a linear relationship between the concentration of the reactants and the rate of reaction. The first-order reaction rate constant for SMX (K_1) was calculated to be 0.042/min. In this context, C_0 represents the pollutant concentration at time zero, Ct is the pollutant concentration at time t, K is the reaction rate constant, and t (in minutes) is the reaction time. Kinetic studies conducted by Zulfiqar et al revealed that the pseudo-first-order reaction model provided the most accurate description of antibiotic degradation behavior.[17] Rapti et al investigated the photocatalytic degradation of pharmaceutical compounds in actual hospital WWTP effluents using a g-C_3N_4 catalyst.[44] Their findings indicated that the degradation process adhered to pseudo-first-order kinetics.

Photocatalytic Degradation of SMX From a Real Hospital Wastewater

To evaluate the applicability of the photocatalytic process for SMX removal in real-world conditions, hospital wastewater known to contain SMX was examined. The physicochemical characteristics of the hospital wastewater were as follows: COD = 365 mg/L, BOD = 172 mg/L, pH = 7.3, and turbidity = 101.5 NTU. Moreover, SMX was spiked into the samples at a concentration of 5 mg/L to facilitate further analysis. Photocatalytic degradation experiments were conducted under optimal conditions determined from previous trials. The results showed that 78% of SMX was removed from the hospital wastewater. This slightly lower efficiency, compared to laboratory conditions, may be attributed to two main factors. First, the presence of suspended and dissolved solids in hospital wastewater can reduce light penetration and photon absorption by the photocatalyst, thereby hindering the generation of reactive oxidative species. Second, the presence of competing organic compounds in the wastewater may lead to the consumption of these oxidizing species, reducing their availability for SMX degradation. Consequently, the overall degradation rate of SMX is decreased in real wastewater matrices.

Conclusion

In this study, G-C_3N_4-CdS was successfully synthesized, and the doping of CdS nanoparticles onto G-C_3N_4 was confirmed using various characterization techniques, including XRD and FE-SEM. These analyses verified the crystalline structure and morphology of the synthesized nanocomposite. Photocatalytic experiments demonstrated that the degradation of SMX followed a first-order kinetic model ($R^2 = 0.995$). Optimal removal conditions were identified as pH 5, a nanocatalyst dosage of 0.7 g/L, a contact time of 60 minutes, and an initial SMX concentration of 5 mg/L. The results indicated enhanced removal efficiency under acidic conditions. Overall, this study highlights that the CdS-modified g-C_3N_4 photocatalyst offers a promising and effective strategy for the treatment of antibiotic-contaminated wastewater, particularly for the removal of SMX.

Acknowledgements

The present project was supported by the Iran University of Medical Sciences (Grant number 95-02-27-28516). The authors express their gratitude to the Research Council for its generous support of this study.

Authors' Contribution

Conceptualization: Ali Esrafily, Mehdi Safari, Majid Kermani, Hossein Pasavand.
Data curation: Ali Esrafily, Hossein Pasavand.
Formal analysis: Ali Esrafily Hossein Pasavand.
Funding acquisition: Ali Esrafily, Hossein Pasavand.
Investigation: Ali Esrafily, Mehdi Safari, Majid Kermani, Hossein Pasavand.
Methodology: Ali Esrafily and Hossein Pasavand.
Project administration: Ali Esrafily.
Resources: Ali Esrafily, Hossein Pasavand.
Software: Ali Esrafily, Hossein Pasavand.
Supervision: Ali Esrafily, Mehdi Safari, Majid Kermani.
Validation: Ali Esrafily, Mehdi Safari, Majid Kermani.
Visualization: Ali Esrafily and Hossein Pasavand.
Writing–original draft: Ali Esrafily, Mehdi Safari, Majid Kermani, Hossein Pasavand.

Writing–review & editing: Ali Esrafily, Hossein Pasavand.

Competing Interests
The authors declared no conflict of interest.

Ethical Approval
There were no ethical considerations to be considered in this research.

Funding
This article was extracted from the MSc thesis of Hossein Pasavand. This study was partially supported by Iran University of Medical Sciences.

Supplementary Files
Supplementary file 1 contains Table S1 and Figures S1-S3.

References
1. Browne AJ, Chipeta MG, Haines-Woodhouse G, Kumaran EP, Hamadani BH, Zaraa S, et al. Global antibiotic consumption and usage in humans, 2000-18: a spatial modelling study. Lancet Planet Health. 2021;5(12):e893-904. doi: 10.1016/s2542-5196(21)00280-1.
2. Llor C, Bjerrum L. Antimicrobial resistance: risk associated with antibiotic overuse and initiatives to reduce the problem. Ther Adv Drug Saf. 2014;5(6):229-41. doi: 10.1177/2042098614554919.
3. Hoseinzadeh E, Alikhani MY, Samargandi MR. Evaluation of synergistic effect of commercial zinc oxide and copper oxide nanoparticles against gram-positive and gram-negative bacteria by fraction inhibitory concentration index. J Adv Med Biomed Res. 2012;20(82):29-41. [Persian].
4. Hoseinzadeh E, Samargandi MR, Alikhani MY, Godini H, Shams Khorramabadi G. Sensitivity coefficient and death kinetics of *Escherichia coli* and *Staphylococcus aureus* to zinc oxide and copper oxide nanoparticles. J Isfahan Med Sch. 2012;30(200):1153-63. [Persian].
5. Kraemer SA, Ramachandran A, Perron GG. Antibiotic pollution in the environment: from microbial ecology to public policy. Microorganisms. 2019;7(6):180. doi: 10.3390/microorganisms7060180.
6. de Ilurdoz MS, Sadhwani JJ, Reboso JV. Antibiotic removal processes from water & wastewater for the protection of the aquatic environment - a review. J Water Process Eng. 2022;45:102474. doi: 10.1016/j.jwpe.2021.102474.
7. Shi J, Dong Y, Shi Y, Yin T, He W, An T, et al. Groundwater antibiotics and microplastics in a drinking-water source area, northern China: occurrence, spatial distribution, risk assessment, and correlation. Environ Res. 2022;210:112855. doi: 10.1016/j.envres.2022.112855.
8. Popoola BM, Ogwerel JP, Oladipo OG. Bacterial isolates from drinking water river sources exhibit multi-drug resistant trait. Environ Monit Assess. 2024;196(11):1054. doi: 10.1007/s10661-024-13117-9.
9. Ovung A, Bhattacharyya J. Sulfonamide drugs: structure, antibacterial property, toxicity, and biophysical interactions. Biophys Rev. 2021;13(2):259-72. doi: 10.1007/s12551-021-00795-9.
10. Zuo R, Liu X, Zhang Q, Wang J, Yang J, Teng Y, et al. Sulfonamide antibiotics in groundwater and their migration in the vadose zone: a case in a drinking water resource. Ecol Eng. 2021;162:106175. doi: 10.1016/j.ecoleng.2021.106175.
11. Sodhi KK, Kumar M, Balan B, Dhaulaniya AS, Shree P, Sharma N, et al. Perspectives on the antibiotic contamination, resistance, metabolomics, and systemic remediation. SN Appl Sci. 2021;3(2):269. doi: 10.1007/s42452-020-04003-3.
12. Plaisance A, Wayment D, Raje H, Boopathy R. Biodegradation of sulfamethoxazole by a bacterium isolated from the Hurricane overtop sediments. Bioresour Technol Rep. 2024;27:101926. doi: 10.1016/j.biteb.2024.101926.
13. Xu D, Xie Y, Li J. Toxic effects and molecular mechanisms of sulfamethoxazole on *Scenedesmus obliquus*. Ecotoxicol Environ Saf. 2022;232:113258. doi: 10.1016/j.ecoenv.2022.113258.
14. Samrot AV, Wilson S, Sanjay Preeth RS, Prakash P, Sathiyasree M, Saigeetha S, et al. Sources of antibiotic contamination in wastewater and approaches to their removal—an overview. Sustainability. 2023;15(16):12639. doi: 10.3390/su151612639.
15. Olasupo A, Ahmed N, Wan Ahmad Kamil WM, Mohd Suah FB. Enhanced removal of sulfamethoxazole antibiotics from aquatic samples by electromembrane extraction process. React Funct Polym. 2022;173:105211. doi: 10.1016/j.reactfunctpolym.2022.105211.
16. Nhoysaykham M, Wu X, Lin Y, Wu S, Li X, Yang C. Efficient removal of antibiotic from aqueous solutions using adsorbent derived from zeolitic imidazolate framework-8. Colloids Surf A Physicochem Eng Asp. 2024;684:133114. doi: 10.1016/j.colsurfa.2023.133114.
17. Zulfiqar N, Nadeem R, Musaimi OA. Photocatalytic degradation of antibiotics via exploitation of a magnetic nanocomposite: a green nanotechnology approach toward drug-contaminated wastewater reclamation. ACS Omega. 2024;9(7):7986-8004. doi: 10.1021/acsomega.3c08116.
18. Wang J, Song J, Zhou Q. In situ-growth of Fe2S3 ultrathin layer on CdS nanorod through cation-exchange for efficient photocatalytic degradation of organic pollutants under visible light coupled oxidant activation. Desalin Water Treat. 2024;319:100434. doi: 10.1016/j.dwt.2024.100434.
19. Yang Z, Yang J, Li L, Cao W, Zhang J, Zhao H, et al. A novel F-BiVO4/g-C3N4/CdS dual S-scheme heterojunction for high-efficient photocatalytic removal of multiple pollutants. Appl Surf Sci. 2024;672:160738. doi: 10.1016/j.apsusc.2024.160738.
20. Hu H, He Y, Wang X, Zhang T, Li D, Sun M, et al. An intermediary route to CdS/Bi2S3 architectures with high-activity and stability in photocatalytic water splitting and dye degradation. Mater Sci Eng B. 2024;305:117431. doi: 10.1016/j.mseb.2024.117431.
21. Li YH, Tang ZR, Xu YJ. Multifunctional graphene-based composite photocatalysts oriented by multifaced roles of graphene in photocatalysis. Chin J Catal. 2022;43(3):708-30. doi: 10.1016/s1872-2067(21)63871-8.
22. Muhmood T, Ahmad I, Haider Z, Haider SK, Shahzadi N, Aftab A, et al. Graphene-like graphitic carbon nitride (g-C3N4) as a semiconductor photocatalyst: properties, classification, and defects engineering approaches. Mater Today Sustain. 2024;25:100633. doi: 10.1016/j.mtsust.2023.100633.
23. Bhanderi D, Lakhani P, Modi CK. Graphitic carbon nitride (g-C3N4) as an emerging photocatalyst for sustainable environmental applications: a comprehensive review. RSC Sustain. 2024;2(2):265-87. doi: 10.1039/d3su00382e.
24. Zubair M, Vanhaecke EM, Svenum IH, Rønning M, Yang J. Core-shell particles of C-doped CdS and graphene: a noble metal-free approach for efficient photocatalytic H2 generation. Green Energy Environ. 2020;5(4):461-72. doi: 10.1016/j.gee.2020.10.017.
25. Liang X, Wang G, Huo T, Dong X, Wang G, Ma H, et al. Band structure modification of g-C3N4 for efficient heterojunction construction and enhanced photocatalytic capability under visible light irradiation. Catal Commun. 2019;123:44-8. doi: 10.1016/j.catcom.2019.01.003.
26. National Center for Biotechnology Information. PubChem Compound Summary for CID 5329, Sulfamethoxazole. 2024. Available from: https://pubchem.ncbi.nlm.nih.gov/compound/Sulfamethoxazole. Retrieved November 18, 2024.

27. Garg R, Gupta R, Bansal A. Synthesis of g-C3N4/ZnO nanocomposite for photocatalytic degradation of a refractory organic endocrine disrupter. Mater Today Proc. 2021;44(Pt 1):855-9. doi: 10.1016/j.matpr.2020.10.787.
28. Afzal MI, Shahid S, Mansoor S, Javed M, Iqbal S, Hakami O, et al. Fabrication of a ternary nanocomposite g-C3N4/Cu@ CdS with superior charge separation for removal of organic pollutants and bacterial disinfection from wastewater under sunlight illumination. Toxics. 2022;10(11):657. doi: 10.3390/toxics10110657.
29. Hoseinzadeh E, Wei C, Farzadkia M, Rezaee A. Effects of low frequency-low voltage alternating electric current on apoptosis progression in bioelectrical reactor biofilm. Front Bioeng Biotechnol. 2020;8:2. doi: 10.3389/fbioe.2020.00002.
30. Hoseinzadeh E, Alikhani MY, Samarghandi MR, Shirzad-Siboni M. Antimicrobial potential of synthesized zinc oxide nanoparticles against gram positive and gram-negative bacteria. Desalin Water Treat. 2014;52(25-27):4969-76. doi: 10.1080/19443994.2013.810356.
31. Balyejjusa S, Adome RO, Musoke D. Spectrophotometric determination of sulphamethoxazole and trimethoprim (co-trimoxazole) in binary mixtures and in tablets. Afr Health Sci. 2002;2(2):56-62.
32. Fu J, Chang B, Tian Y, Xi F, Dong X. Novel C3N4–CdS composite photocatalysts with organic–inorganic heterojunctions: in situ synthesis, exceptional activity, high stability and photocatalytic mechanism. J Mater Chem A. 2013;1(9):3083-90. doi: 10.1039/c2ta00672c.
33. Chen L, Xu Y, Chen B. In situ photochemical fabrication of CdS/g-C3N4 nanocomposites with high performance for hydrogen evolution under visible light. Appl Catal B Environ. 2019;256:117848. doi: 10.1016/j.apcatb.2019.117848.
34. Sapińska D, Adamek E, Masternak E, Zielińska-Danch W, Baran W. Influence of pH on the kinetics and products of photocatalytic degradation of sulfonamides in aqueous solutions. Toxics. 2022;10(11):655. doi: 10.3390/toxics10110655.
35. Song Y, Tian J, Gao S, Shao P, Qi J, Cui F. Photodegradation of sulfonamides by g-C3N4 under visible light irradiation: effectiveness, mechanism and pathways. Appl Catal B Environ. 2017;210:88-96. doi: 10.1016/j.apcatb.2017.03.059.
36. Wang L, Wang Y, Wang Y, Wang H, Wu H, Gao D. Efficient photocatalytic degradation of sulfonamides in wastewater using g-C3N4 heterostructures: a critical review. Environ Technol Innov. 2024;36:103854. doi: 10.1016/j.eti.2024.103854.
37. Boreen AL, Arnold WA, McNeill K. Photochemical fate of sulfa drugs in the aquatic environment: sulfa drugs containing five-membered heterocyclic groups. Environ Sci Technol. 2004;38(14):3933-40. doi: 10.1021/es0353053.
38. Ioannidou E, Frontistis Z, Antonopoulou M, Venieri D, Konstantinou I, Kondarides DI, et al. Solar photocatalytic degradation of sulfamethoxazole over tungsten–modified TiO2. Chem Eng J. 2017;318:143-52. doi: 10.1016/j.cej.2016.06.012.
39. Khataee A, Darvishi Cheshmeh Soltani R, Hanifehpour Y, Safarpour M, Gholipour Ranjbar H, Joo SW. Synthesis and characterization of dysprosium-doped ZnO nanoparticles for photocatalysis of a textile dye under visible light irradiation. Ind Eng Chem Res. 2014;53(5):1924-32. doi: 10.1021/ie402743u.
40. Anandan S, Kathiravan K, Murugesan V, Ikuma Y. Anionic (IO3-) non-metal doped TiO2 nanoparticles for the photocatalytic degradation of hazardous pollutant in water. Catal Commun. 2009;10(6):1014-9. doi: 10.1016/j.catcom.2008.12.054.
41. Sarafraz M, Sadeghi M, Yazdanbakhsh A, Amini MM, Sadani M, Eslami A. Enhanced photocatalytic degradation of ciprofloxacin by black Ti3+/N-TiO2 under visible LED light irradiation: kinetic, energy consumption, degradation pathway, and toxicity assessment. Process Saf Environ Prot. 2020;137:261-72. doi: 10.1016/j.psep.2020.02.030.
42. Mahmoodi F, Jalilzadeh Yengejeh R, Tirgir F, Sadeghi M. Removal of 1-naphthol from water via photocatalytic degradation over NS-TiO2/silica sulfuric acid under visible light. J Adv Environ Health Res. 2022;10(1):59-72. doi: 10.32598/jaehr.10.1.1242.
43. Rezaei S, Maleki A, Rezaee R, Kashefi H, Zandsalimi Y. Enhancement of photocatalytic removal of 4-chlorophenol from aqueous solutions by manganese oxide doped ZnO nanoparticles using RSM. J Adv Environ Health Res. 2024;12(4):205-11. doi: 10.34172/jaehr.1365.
44. Rapti I, Kourkouta T, Malisova EM, Albanis T, Konstantinou I. Photocatalytic degradation of inherent pharmaceutical concentration levels in real hospital WWTP effluents using g-C3N4 catalyst on CPC pilot scale reactor. Molecules. 2023;28(3):1170. doi: 10.3390/molecules28031170.